Desalination and Water Treatment
www.deswater.com

doi:10.5004/dwt.2017.21380

88 (2017) 67–74
September

Biological nutrient removal and fouling behavior in an UCT-MBR process: synergistic effects of aeration intensity and mixed liquor recycling ratio

Zhaozhao Wang[a], Kai Zhang[a], Changwen Wang[b], Lina Yan[c], Wei Zhang[a], Fengbing Tang[a], Simin Li[a,*]

[a]*College of Energy and Environmental Engineering, Hebei University of Engineering, Handan, 056038, China, Tel. +8618303233729, email: W-Z-Z@163.com (Z. Wang), hebeizuiqingfeng@163.com (K. Zhang), zhangwei1981@hebeu.edu.cn (W. Zhang), fbtang1004@163.com (F. Tang), 18303233729@163.com (S. Li)*
[b]*College of Resources and Environment, Linyi University, Linyi, 276000, China, email: wangchangwen@lyu.edu.cn (C. Wang)*
[c]*Graduate School, Hebei University of Engineering, Handan 056038, China, email: yanlina01@126.com (L. Yan)*

Received 17 March 2017; Accepted 27 August 2017

ABSTRACT

A bench-scale university of cape town-membrane bioreactor (UCT-MBR) process was operated treating real municipal wastewater with reference to the synergistic effects of aeration intensity and mixed liquor recycling ratio on biological nutrient removal performance and membrane fouling propensity. Results showed that chemical oxygen demand (COD) and NH_4^+-N removal was slightly dependent on variations in aeration intensity and recycling ratio. The increase in recycling ratio strengthened the enrichment of denitrifying poly-phosphate accumulating organisms (DPAOs) and the anoxic dephosphorization efficiency. The largest ratio of DPAOs to poly-phosphate accumulating organisms (PAOs) (50.7%) could be obtained when a low aeration intensity (100–125 L/h) and the highest recycling ratio (r_1: 400%) were demonstrated. In contrast, a higher aeration intensity level (250–300 L/h) resulted in the deterioration of the anoxic dephosphorization efficiency, decreasing to 78%, 77.03% and 70% from 93%, 92.6% and 79.6% (r_1 from 400% to 200%), respectively. The bio-cake resistance was significantly reduced by a higher aeration intensity notwithstanding higher concentrations of extracellular polymeric substances (EPS). The combined shear forces induced by these two parameters promoted the smaller-size particles and higher concentrations of soluble microbial products (SMP) in the bulking sludge which resulted in the increased resistance of deep pore clogging. Fourier transform infrared spectroscopy (FT-IR) analysis revealed that variations in these two parameters had no effect on the main composition of organic matters in the membrane foulants.

Keywords: Membrane bioreactor; Aeration intensity; Mixed liquor recycling ratio; Denitrifying dephosphorization; Membrane fouling

1. Introduction

Membrane bioreactor (MBR) is a biological wastewater treatment process coupling with membrane filtration technology instead of gravitational settling, which is always used for solid-liquid separation in conventional wastewater processing. The excellent quality of produced effluent has resulted in MBR being increasingly used for waster reuse and reclamation [1]. Furthermore, various biological nutrient removal (BNR) processes have been developed based on MBR, for enhancing biological nitrogen and phosphorus removal, made necessary by the extravagant water-body eutrophication [2–4]. The enhanced biological phosphorus removal membrane bioreactor process (EBPR-MBR) has been widely applied for simultaneous nitrogen and phosphorus removal in municipal wastewater treatments. Nevertheless, membrane fouling is still a major obstacle for the sustainable process operation, significantly increasing operation and maintenance (O & M) costs. To date, various different BNR-MBR configurations and process conditions

*Corresponding author.

have been investigated, to determine their specific membrane fouling behaviors and mechanisms [5–7].

Multiple authors have used shear stress induced by the scouring aeration of the membrane surface in an attempt to mitigate membrane fouling. Braak et al. reported that increased aeration intensity substantially prevented the formation of the bio-cake which alleviated membrane fouling effectively in a submerged MBR system. Moreover, aeration intensity was also found to have a significant impact on biomass properties (*i.e.* particle size distribution, biopolymer production) [8]. Meng et al. revealed that the colloidal fraction of bulking sludge increased and sludge particle size decreased when the aeration intensity varied from 150 to 800 L/h [9]. However, most previous studies mainly focused on the effects of aeration intensity on membrane fouling behaviors in a submerged membrane bioreactor for organic contaminants and ammonia removal. There would be certain conflicting influences on enhancing biological nutrient removal, while reducing fouling if aeration would be performed at high intensity. Generally, the dissolved oxygen (DO) in the bulking sludge increases when higher aeration intensity is used. In the BNR-MBR process, increased aeration intensity for fouling reduction can also increase the DO level, which favors the nitrification bioprocess, but affects denitrification due to the recycling of mixed liquor from the aerobic tank [10]. However, increased recycling ratio can generate more shear stresses, which results in the destruction of microbial flocs [11]. It is crucial to gain more insight into the combined effects of the aeration intensity and recycling ratio in order to achieve better biological nutrient removal and alleviate the membrane fouling.

In the present study, a submerged membrane bioreactor with a UCT configuration was operated to investigate the combined effects of two key operating parameters (aeration intensity and mixed liquor recycling ratio) on BNR performance and membrane fouling behaviors. The efficiency of the anoxic dephosphorization was also investigated, to examine the dynamic succession of PAOs and DPAOs. Moreover, biomass properties, such as sludge particle size distribution, extracellular polymeric substances (EPS) and soluble microbial products (SMP), were analyzed to describe the membrane fouling mechanisms. The biopolymer deposited on the membrane surface was further characterized by FT-IR analysis.

2. Materials and methods

2.1. Experimental set-up and operational conditions

The bench-scale plant (Fig. 1) comprised a bioreactor (total volume 28 L) with UCT configuration: anaerobic tank (20% of the total volume), anoxic tank-1 (20%) and anoxic tank-2 (20%) with mechanical mixtures, followed by an aerobic tank (40%) with one submerged flat-sheet membrane (Kubota corporation: chlorinated polyethylene; pore size: 0.4 μm; surface area: 0.1 m^2). A pH-DO sensor (WTW Multi 340i, Germany) was fitted to monitor the DO levels in the aerobic membrane tank. The temperature was maintained at 20–23°C by a heater. The plant was provided with a programmable logic controller (PLC) and data acquisition system that controlled the flows of all the streams. The membrane was operated at a flux of 20 L/(m^2·h), with intermittent suction (9-min suction and 1-min relaxation). Wastewater was pumped from the storage tank to the anaerobic tank, followed by the anoxic tank-1, anoxic tank-2, and the aerobic membrane tank, and finally pumped out through the membrane module. The recycling overflow from the aerobic tank to the anoxic tank-1 (r_1) and the recycling flow from the anoxic tank-2 to the anaerobic tank (r_2) were achieved using a sludge lift pump and a recycling pump, respectively. The hydraulic retention time (HRT) was 15.5 h and a target sludge retention time (SRT) of 20 d was maintained through direct daily discharge of waste sludge from the aerobic tank. The mixed liquor suspended solids (MLSS) in the aerobic membrane tank was maintained at approximately 5000 mg/L.

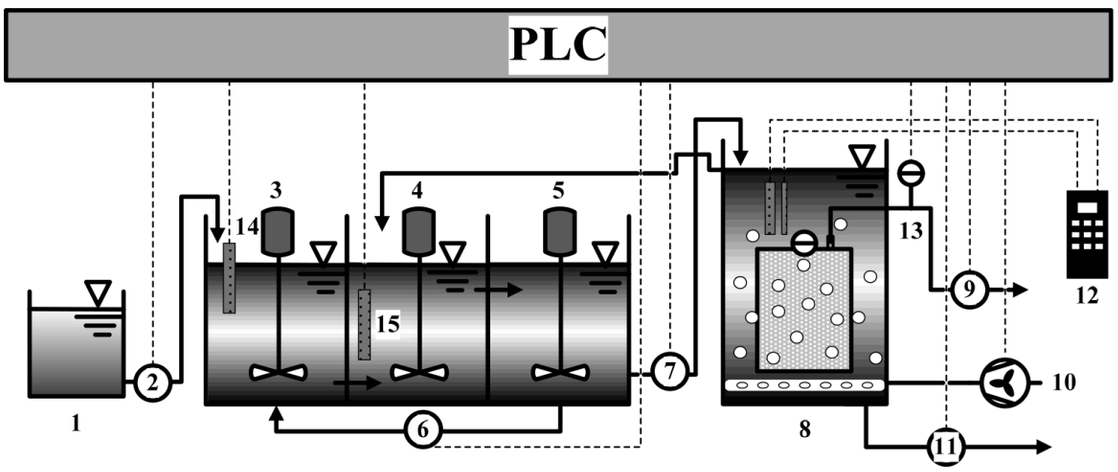

1 storage tank; 2 influent pump; 3 anaerobic tank; 4 anoxic tank-1; 5 anoxic tank-2; 6 recycling pump; 7 sludge lift pump; 8 aerobic membrane tank; 9 permeate pump; 10 air compressor; 11 sludge discharge pump; 12 DO/pH; 13 pressure guage; 14 water level controller; 15 heater.

Fig. 1. Flow diagram of the bench-scale UCT-MBR process.

2.2. Characteristics of feeding wastewater and seed sludge

The UCT-MBR plant was fed with real municipal sewage water (COD, 296.7 ± 29.6 mg/L; NH_4^+-N, 49.9 ± 4.5 mg/L; total nitrogen (TN), 50.2 ± 4.5 mg/L; total phosphorus (TP), 6.04 ± 0.95 mg/L; COD/TN/TP, 49.1/8.3/1), and the seed sludge was taken from the East wastewater treatment plant of Handan, Hebei Province, which employs a T-type oxidized ditch process, achieving satisfactory biological nitrogen removal. After one month of sludge acclimation, a stable performance was achieved and experiments commenced according to the operational procedures shown in Table 1. The fouled membrane module was taken out from the aerobic tank, flushed with pure water and soaked in NaClO solution (0.5%) for 24 h, to recover the membrane permeability at the end of each cycle.

2.3. Analytical methods

2.3.1. Wastewater and sludge analyzes

COD, NH_4^+-N, NO_3^--N, NO_2^--N, TN, TP, PO_4^{3-}-P, MLSS, and mixed liquor volatile suspended solids (MLVSS) were measured according to standard methods [12].

2.3.2. PAOs/DPAOs assays and evaluation of anoxic dephosphorization efficiency

The metabolic kinetic activities of PAOs under aerobic conditions and of DPAOs under anoxic conditions were determined using the method proposed by Wachtmeister et al. [13]. The batch tests were conducted in a 1 L sequencing batch reactor (SBR) with temperature controller (21 ± 1°C). The pH was maintained at approximately 7.2, by adding hydrochloric acid. Waste sludge (800 mL) was washed for 5 min with distilled water to remove the ortho-phosphate in the bulk liquid. After that, the sludge was incubated, under anaerobic conditions, with sodium acetate for 4 h. The anaerobic sludge was then divided into two parts. One part was exposed to aerobic conditions with DO (1.5–2.5 mg/L), whilst the other was exposed to anoxic conditions with NO_3^--N (50 mg/L), for 4 h, respectively. K_{aer} and K_{ano} were the maximum values of specific phosphorus uptake rate under aerobic and anoxic conditions, respectively. K_{aer} and K_{ano} were measured and compared, at the end of different operational periods.

The anoxic dephosphorization efficiency was calculated using Eq. (1):

Table 1
Operational parameters throughout the operations

Operational periods	Recycling ratio (r_1)	Recycling ratio (r_2)	Aeration intensity/ (L/h)	DO / (mg/L)
RUN I	200%	100%	100 – 125	1~2
RUN II	300%	100%	100 – 125	1~2
RUN III	400%	100%	100 – 125	1~2
RUN IV	200%	100%	250 – 300	2~4
RUN V	300%	100%	250 – 300	2~4
RUN VI	400%	100%	250 – 300	2~4

$$T = 1 - \frac{(1+r_1+r_2)c_{\text{ano2}}}{(1+r_2)c_{\text{ana}}+r_1c_{\text{aer}}} \quad (1)$$

where C_{ana}, C_{ano2}, C_{aer} refer to the effluent phosphate concentrations in the anaerobic, anoxic (tank-2) and aerobic membrane tanks, respectively; T indicates that the phosphate in the effluent of both the anaerobic tank and the internal recycle (r_1) was removed from the anoxic tanks.

2.3.3. Evaluation of fouling resistance and fouling rate

Specific membrane resistance was evaluated by the resistance-inseries model, using Eq. (2):

$$J=\frac{TMP}{\mu R_t}=\frac{TMP}{\mu\left(R_c+R_p+R_m\right)} \quad (2)$$

where J, μ refer to the permeate flux (L/(m²·h)) and water dynamic viscosity (N·s/m²), respectively. The transmembrane pressure (TMP) value was corrected for water viscosity changes due to the temperature variations, as recommended by Rosenberger et al. [14], with 20°C as the reference temperature. The experimental procedure to obtain each fouling resistance value was as follows: (a) the resistance of the membrane (R_m) was estimated by measuring the water flux of de-ionized (DI) water; (b) the total resistance (R_t) was evaluated by the final flux of sludge wastewater microfiltration; (c) the membrane surface was then flushed with water and cleaned with a sponge to remove the bio-cake. Subsequently, the DI water flux was re-measured to obtain the resistance of $R_p + R_m$. The pore clogging resistance (R_p) was calculated from steps (a) and (b), and the cake resistance (R_c) obtained from (b) and (c).

Fouling rate (F_r, kPa/d) was calculated as the difference in the TMP at 20th day (TMP_{end}) and 1st day (TMP_{start}) of each operational period using Eq. (3):

$$F_r=\frac{TMP_{\text{end}}-TMP_{\text{start}}}{\Delta t} \quad (3)$$

2.3.4. EPS and SMP analysis

The extraction of EPS was based on a cation ion exchange resin (CER, Dowex-Na form) method [15]: 50 mL sludge suspension was taken and centrifuged at 5000×g for 5 min, at 4°C. Next SMP was obtained by filtering the supernatant through a 0.45 μm membrane filter. After that, the sludge pellets were resuspended to their original volume, using a buffer consisting of 2 mM Na_3PO_4, 4 mM NaH_2PO_4, 9 mM NaCl and 1 mM KCl, at pH 7. The sludge was then transferred to an extraction beaker with baffles and the CER (70 g/g MLSS) added. The suspension was stirred with the selected stirring intensity (800 rpm) and extraction time (2 h), at 4°C. The selected EPS was harvested by centrifugation of a sample of the CER/sludge suspension for 1 min, at 12,000×g, performed to remove the CER. The supernatant was centrifuged twice for 15 min at 12,000×g, at 4°C, in order to remove remaining floc components. Bound EPS was obtained by filtering the supernatant through a 0.45 μm membrane filter. The SMP and bound EPS were normalized as the sum of carbohydrate and protein, which were analyzed using the

phenol/sulfuric-acid method and the folin method [16], respectively.

2.3.5. Particle size and FT-IR analysis

The particle size distribution of the activated sludge from the aerobic membrane tank was measured using a Mastersizer counter (Marlvern 2000, UK).

The fouled membrane module was taken out from the aerobic tank and flushed with pure water once each cycle was terminated. Approximately 300 mL washed liquid was taken and placed in a dryer at 105°C for 24 h, to obtain dry foulants. An FT-IR spectrometer (FT-IR 6700, USA) was used to characterize the major functional groups of organic matters in the membrane foulants. KBr pellets, containing 0.5% (dry powder) of the sample, were prepared and examined using the FT-IR spectrophotometer. The spectrum was calculated as the average of 256 scans, with the wave number ranging from 4000 to 400 cm^{-1}, at a resolution of 4 cm^{-1}.

3. Results and discussion

3.1. Performance of organic contaminants and nutrient removal

3.1.1. Removal of organic contaminants

The performance of COD removal at different aeration intensities and recycling ratios was depicted in Fig. 2. It can be seen that either the aeration intensity or the recycling ratio had a slight impact on COD removal. The COD concentration in the influent distinctly fluctuated between 247 and 370 mg/L, and was reduced to approximately 41.97 mg/L in the aerobic tank after going through the anaerobic, anoxic and aerobic tanks. A final 10 mg/L reduction in soluble COD levels, which resulted from the membrane filtration, was observed in this study, with the average removal efficiency of COD at 89.4%. The average COD concentration in the supernatant in RUN IV–VI was approximately 10 mg/L higher than that in RUN I–III, which implies, compared with the recycling ratio, that the increased aeration intensity had a more significant impact on the release of colloidal COD and microbial metabolic productions.

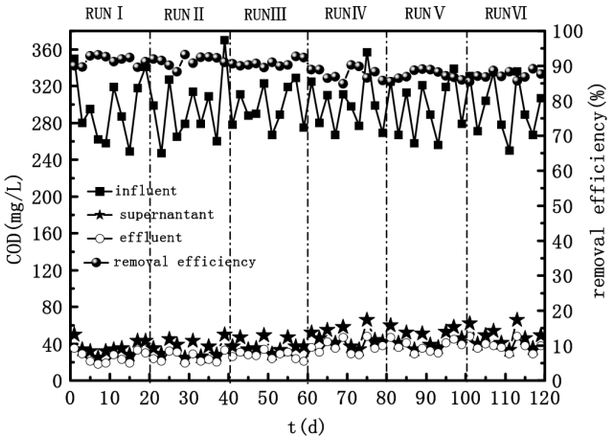

Fig. 2. Performance of COD removal during operations.

3.1.2. Nitrogen removal

Fig. 3 presents the performance of nitrogen removal in UCT-MBR throughout the entire experiments. It can be clearly seen that the NH_4^+-N concentration in effluent was stabilized at approximately 0.14 mg/L, with an average removal efficiency of 99.7%, implying that ammonia removal was independent of aeration intensity and recycling ratio. The DO concentration was maintained above 1 mg/L, which was sufficient for the nitrifiers to complete the nitrification bioprocesses. Interestingly, the TN removal was observed to be dependent on both aeration intensity and nitrate recycling ratio. The TN concentration in the influent was approximately 50.45 mg/L and the removal efficiency of TN ranged from 64% to 79.5% when the recycling ratio increased from 200% to 400% in RUN I-III, which indicates that a higher recycling ratio favors TN removal, due to the increased amount of oxidized ammonia (mainly into nitrate). The average removal efficiency of TN was approximately 71.56%, with a TN concentration of 14.35 mg/L in the effluent.

In contrast, TN removal was always lower in RUN IV-VI, under the corresponding recycling ratio in RUN I-III, with an average removal efficiency of 70%. More specifically, a higher aeration intensity resulted in a decreased removal efficiency by 6.97%, 5.36%, and 9.13%, respectively, at the corresponding recycling ratios. The higher DO level that was carried in the mixed liquor recycling flow destroyed the anoxic environment for denitrification, thus impairing TN removal. It is known that DO can compete with oxidized ammonia to obtain electron donors for deoxidized bioreactions, especially when the existing carbon source is limited. In a previuos study, Tan and Ng also found that when using the same recycling ratio, higher DO levels consume more of the available carbon sources, which, in turn, reduces the provisions of denitrifying electron donors, thus exacerbating the overall performance of TN removal in an anoxic/aerobic-membrane bioreactor process [10].

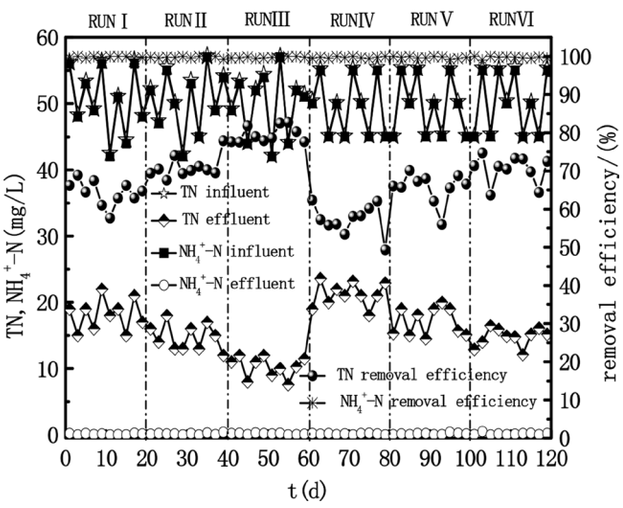

Fig. 3. Performance of NH_4^+-N and TN removal during operations.

3.1.3. Phosphorus removal

The performance of TP removal throughout the operational periods was shown in Fig. 4. The average TP concentrations in the influent were 6.06, 5.95 and 6.1 mg/L from RUN I to RUN III, with removal efficiencies of 58.04%, 73.52% and 92.56%, respectively, which were higher than those obtained under the corresponding recycling ratios from RUN IV to RUN VI. The TP removal efficiency increased with the increase in recycling ratio, under both high and low DO levels, which indicates that the mixed liquor recycling ratio always exhibited a positive impact on TP removal. The highest removal efficiency of TP (92.56%) was achieved when a low DO level and the highest recycling ratio were demonstrated (shown in RUN III). In contrast, the high DO level resulted in the reduction of TP removal to 77%, under the same recycling ratio (shown in RUN VI), implying that the high DO level had a negative impact on TP removal. It was also observed that combined effects of the lowest recycling ratio (200%) and a high DO level resulted in the lowest removal efficiency of TP (41.1%, RUN IV).

The combined effects of aeration intensity and recycling ratio on the evolutions of DPAOs, PAOs and anoxic dephosphorization efficiency were shown in Fig. 5. It can be clearly seen that both K_{aer} and K_{ano} values increased in RUN I-III and RUN IV-VI, revealing that the recycling ratio strengthened the enrichments of PAOs and DPAOs. Furthemore, the DPAOs activity increased faster than that of the PAOs, with the ratio of DPAOs to PAOs and the T value increasing from 31% to 50.7% and 38% to 93%, respectively, under the respective recycling ratio (r_1 from 200% to 400%), in RUN I-III. In contrast, the ratio of DPAOs to PAOs only increased from 26.6% to 40.2%, with the T value increasing from 24% to 78% under the corresponding recycling ratio in RUN IV-VI, which proves that the enriching rates of DPAOs and PAOs decreased due to the high DO level.

Fig. 6 plots the removal efficiency of total nitrogen (TN_{re}) and the concentration of total nitrogen in the effluent (TN_{eff}) as a function of the removal efficiency of total phosphorus (TP_{re}) and the concentration of total phosphorus in the effluent (TP_{eff}), respectively. A higher TN removal efficiency was obtained when a higher TP removal efficiency was achieved. Furthermore, the changing trend of TN_{eff} was similar to that of TP_{eff}. The positive linear correlations between TN_{re} and TP_{re}, and TN_{eff} and TP_{eff} were expressed using Eqns. (4) and (5), respectively:

$$TN_{eff} = 2.76TP_{eff} + 10.46\, R_1^{\,2} = 0.636 \tag{4}$$

$$TN_{re} = 3.58TP_{re} + 44.11\, R_2^{\,2} = 0.679 \tag{5}$$

In simultaneous nitrogen and phosphorus removal processes, a competition for carbon sources exists between heterotrophic denitrifiers and PAOs. DPAOs can ease the requirements of electron donors by using poly-β-hydroxybutyrate (PHB) as the carbon source for simultaneous dentrification and phosphorus uptake, which markedly impact on TN and TP removal. The similar changing trends between TN_{re} and TP_{re}, and TN_{eff} and TP_{eff} could be explained by the behaviors of DPAOs and the denitrifying dephos-

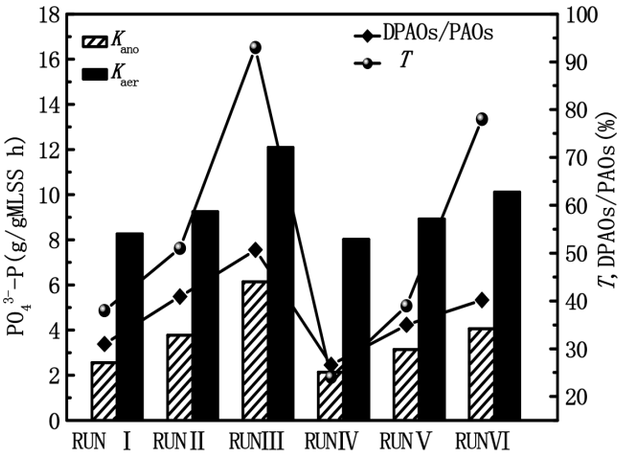

Fig. 5. Evolution of PAOs, DPAOs and anoxic dephosphorization.

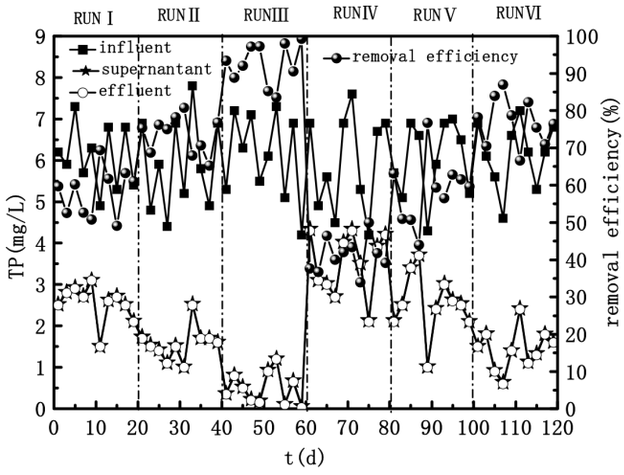

Fig. 4. Performance of TP removal during operations.

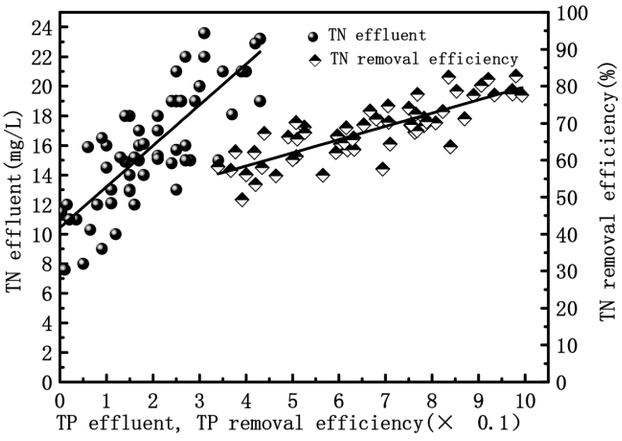

Fig. 6. Correlations between TN_{re} and TP_{re}, TN_{eff} and TP_{eff}.

phorization efficiency. The TN and TP removal was higher when the enrichment of DPAOs and enhancement of anoxic dephosphorization efficiency were achieved, and *vice versa*.

3.2. Membrane fouling

3.2.1. Membrane fouling behaviors

The membrane fouling behaviors observed during the six operational periods are presented in Fig. 7. It is obviously that the fouling rates were higher in RUN I-III (2.9–3.25 kPa/d) than that in RUN IV-VI (1.0–1.4 kPa/d), confirming that a higher aeration intensity results in a lower fouling rate. Each resistance term was analyzed to examine the fouling tendencies (summarized in Table 2). Normally, two opposite actions exist for controlling the bio-cake formation rate: permeation drag, which is generated by permeate flux, increased with operation TMP and back transport, consistent of Brownian diffusion and inertial lift, and shear-induced diffusion [17]. It was observed that bio-cake resistances in RUN I-III (72.8–77.5 (10^{11}/m)) were higher than those in RUN IV-VI (18.7–22.4 (10^{11}/m)), which suggests that the shear force generated by high aeration intensity can effectively remove foulants deposited on the membrane surface (Table 2). Furthermore, the contribution of bio-cake resistance to total resistance ranged between 78.3% and 83.2% in RUN I-III, and 57.3% and 58.6% in RUN IV-VI, which proves that the contribution of bio-cake resistances to membrane fouling decreased when a higher aeration intensity was used although it was still the main determinant of membrane fouling. The R_p value and the ratio of R_p to R_t increased from 6.85 to 11.1 (10^{11}/m) (8.2%–17.1%) in RUN I-III and from 8.95 to 13.95 (10^{11}/m) (28.1%–32.7%) in RUN IV-VI, revealing that metabolic productions and colloidal particles that contribute to irreversible fouling resistance played an increasingly important role in membrane fouling behaviors.

3.2.2. Particle size distribution of aerobic activated sludge

In this study, the membrane fouling degrees, observed in the different operational periods, mainly resulted from differences in shear forces and variations in biomass properties. In addition to the scouring effect on the membrane surface, higher aeration intensity also exhibits shear stresses on sludge flocs [9]. Moreover, the sludge flocs can also be destroyed in a high recycling system due to shear stresses resulted from the high flow velocity [11]. Fig. 8 presents the size distributions of aerobic activated sludge particles during the six operational periods. It can be observed that either increased aeration or recycling ratio could result in a

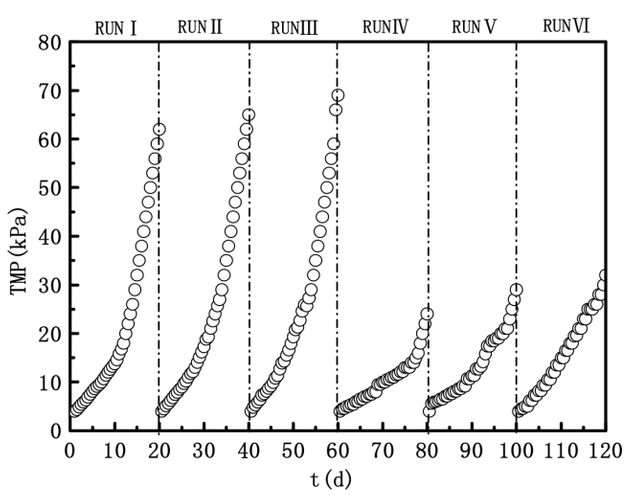

Fig. 7. TMP variations during operations.

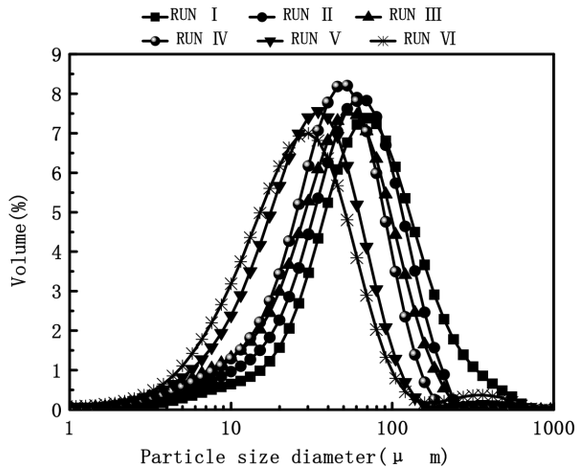

Fig. 8. Particle size distribution of the aerobic activated sludge during operations.

Table 2
Distributions of membrane filtration resistances during operations

Operational periods	Items(%)			
	R_c/(10^{11}/m)	R_p/(10^{11}/m)	R_m/(10^{11}/m)	R_t/(10^{11}/m)
RUN I	72.8 (83.2)	6.85 (8.2)	4.25 (5.1)	83.9
RUN II	77.1 (81.1)	9.25 (10.2)	4.25 (4.7)	90.6
RUN III	77.55 (78.3)	11.1 (17.1)	4.25 (4.6)	91.9
RUN IV	18.7 (58.6)	8.95 (28.1)	4.25 (13.3)	31.9
RUN V	22.5 (58.4)	11.8 (30.6)	4.25 (11)	38.6
RUN VI	24.4 (57.3)	13.95 (32.7)	4.25 (10)	42.6

decrease in size of sludge particles, which further confirms that the destruction of sludge flocs originated from the combined shear effects. The largest sludge particles were observed in RUN I (d (0.5): 73.4 μm), whereas the smallest ones, in RUN VI (d (0.5): 27.4 μm).

3.2.3. EPS and SMP productions

Apart from the shear effects on particle size distributions, the aeration intensity and recycling ratio also exercised substantial effects on microbial metabolites. The variations in the concentrations of EPS and SMP are shown in Fig. 9. Results indicate that carbohydrates were the dominant components in both EPS and SMP. The concentrations of EPS and SMP were higher in RUN IV-VI than in RUN I-III, under the corresponding recycling ratios, indicating that microbial metabolites increased with the increase in aeration intensity, which would appear to be in agreement with previous findings [8,9]. Moreover, the concentrations of EPS and SMP also increased with the recycling ratio. The EPS concentration increased by 22.8% and 24.8%, when the recycling ratio increased from 200% to 400% , in RUN I-III and RUN IV-VI, respectively, during which the ratio of the carbohydrate fraction of EPS (EPS_c) to the protein fraction of EPS (EPS_p) decreased to 3.77 and 3.55 from 4.66 and 4.5, respectively. Meanwhile, the average concentrations of carbohydrate fraction of SMP (SMP_c) and protein fraction of SMP (SMP_p) in RUN IV-VI increased by 10.8% and 40.7% , respectively, from those in RUN I-III. The SMP can be readily deposited onto the membrane surface by permeation drag and is not readily detached by shear force due to its low back-transport velocity, which leads to irreversible membrane fouling [18]. A high aeration intensity combined with the highest recycling ratio (RUN VI) resulted in the largest amount of SMP, which contributed to the highest resistance of deep pore clogging (Table 2, Section 3.2.1).

However, it was previously reported that higher EPS concentrations could cause higher bio-cake resistance [19], which is inconsistent with the results obtained in this study. The R_c values in RUN IV-VI were lower than those in RUN I-III (as discussed in section 3.2.1). Therefore, it can be deduced that shear stress induced by a high aeration intensity could scour the membrane surface effectively and generate high back-transport velocity for bio-solids, which would reduce the amount of EPS matrix dragged by the permeate flux to deposit on the membrane surface.

3.2.4. FT-IR analysis of membrane foulants

The FT-IR spectra of foulants deposited on the membrane surface during the different operational periods are presented in Fig. 10. They are similar in profile, which indicates that the aeration intensity and recycling ratio had no effects on biopolymers composition. The spectrum shows a broad region of absorption at 3416 cm^{-1}, which is due to the stretching of the O-H bond in the hydroxyl functional groups, peaking at 2924 cm^{-1}, which might be explained by the stretching of C-H bonds [20]. As evidenced by Fig. 10, there are two peaks (1654 and 1546 cm^{-1}) in the spectrum, which are unique to secondary protein structures, known as amides I and II [21]. In addition, a broad peak at 1047 cm^{-1} exhibits the character of carbohydrates or carbohy-

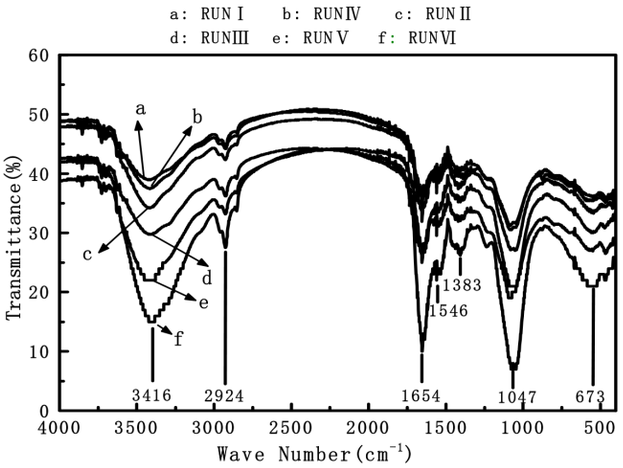

Fig. 10. FT-IR spectra of membrane foulants during operations.

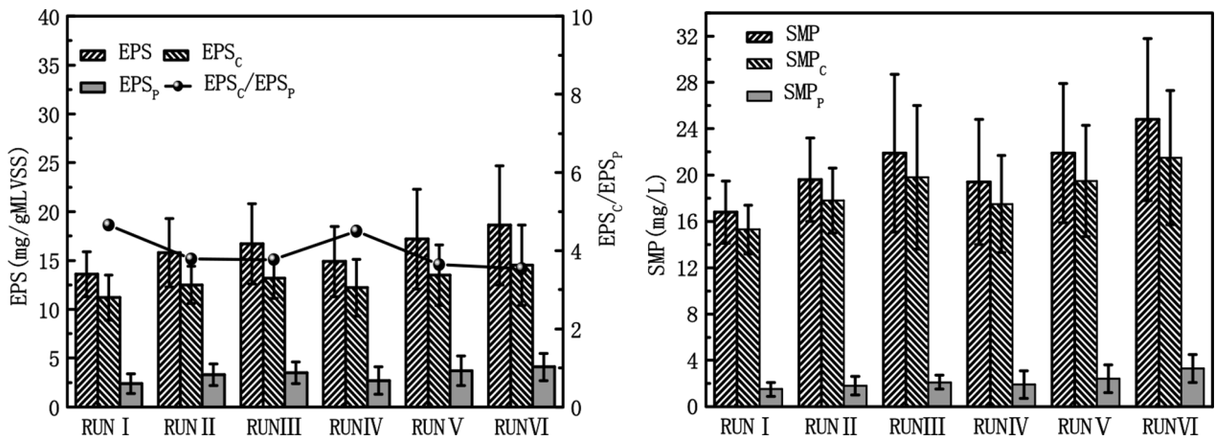

Fig. 9. Variations in the concentrations of (a) EPS and (b) SMP.

drate-like substances [22]. These results indicate that proteins and carbohydrates are part of the membrane foulants. Based on the peak at 1383 cm^{-1}, it can be concluded that the membrane foulants contained a certain amount of lipids [23]. The functional groups indicated by the sharp peak at 673 cm^{-1}, which belongs to the finger print region, could hardly be determined. From Fig. 10 it can also be seen that the absorption intensities of the FT-IR spectrums, in the six operational periods, were different from each other. The absorption intensity could reflect the relative amount of biopolymers in the total foulants. The intensities were given in the order of: RUN IV > RUN V > RUN III > RUN II > RUN IV > RUN I, which coincided with results discussed in section 3.2.3.

4. Conclusion

Under the processed conditions, the main findings are summarized as follows: (1) aeration intensity and mixed liquor recycling ratio exhibited significant influences on TN and TP removal but only slight impacts on removal of organic contaminants and NH_4^+-N. The increase in recycling ratio (r_1 from 200% to 400%) strengthened the enrichment of DPAOs and anoxic dephosphorization efficiency. The highest removal efficiencies of TN and TP (79.5% and 92.56%, respectively) as well as the largest fraction of DPAOs among the populations of PAOs (50.7%), could be obtained simultaneously when a low aeration intensity and the highest recycling ratio were demonstrated. (2) The bio-cake resistance was significantly reduced by a higher aeration intensity, notwithstanding the higher EPS production. The combined shear forces induced by the aeration intensity and recycling ratio resulted in smaller-size particles and higher amount of SMP in the bulking sludge, which resulted in the increased resistance of deep pore clogging. (3) A higher recycling ratio tended to induce higher ratio of EPS_p/EPS_c, whereas the FT-IR analysis revealed that the variations in aeration intensity and recycling ratio had no effect on the main composition of membrane organic foulants.

Acknowledgements

This work was financially supported by Major Science and Technology Program for Water Pollution Control and Treatment of China(2012ZX07314-008), Colleges and Universities in Hebei Province Science and Technology Research Projects (QN2015115), Doctoral Degree Construction Program of Hebei University of Engineering(16964213D), Hebei Provincial Natural Science Fund Project (E2016402017).

References

[1] S. Judd, The status of industrial and municipal effluent treatment with membrane bioreactor technology, Chem. Eng. J., 305 (2016) 37–45.
[2] H. Lee, J. Han, Z. Yun, Biological nitrogen and phosphorus removal in UCT-type MBR process, Water Sci. Technol., 59 (2009) 2093–2099.
[3] B. Lesjean, R. Gnirss, C. Adam, Process configurations adapted to membrane bioreactors for enhanced biological phosphorous and nitrogen removal, Desalination, 149 (2002) 217–224.
[4] H. Monclús, J. Sipma, G. Ferrero, I. Rodriguez-Roda, Optimization of biological nutrient removal in a pilot plant UCT-MBR treating municipal wastewater during start-up, Desalination, 250 (2010) 592–597.
[5] M. Paetkau, N. Cicek, Comparison of nitrogen removal and sludge characteristics between a conventional and a simultaneous nitrification-denitrification membrane bioreactor, Desalination, 283 (2011) 165–168.
[6] H. Shin, S. Kang, Performance and membrane fouling in a pilot scale SBR process coupled with membrane, Water Sci. Technol., 47 (2003) 139–144.
[7] E. McAdam, S. Judd, E. Cartmell, B. Jefferson. Influence of substrate on fouling in anoxic immersed membrane bioreactors, Water Res., 17 (2007) 3859–3867.
[8] E. Braak, M. Alliet, S. Schetrite, C. Albasi, Aeration and hydrodynamics in submerged membrane bioreactors, J. Membr. Sci., 379 (2011) 1–18.
[9] F. Meng, F. Yang, B. Shi, H. Zhang, A comprehensive study on membrane fouling in submerged membrane bioreactors operated under different aeration intensities, Separ. Purif. Technol., 59 (2008) 91–100.
[10] T.W. Tan, H.Y. Ng, Influence of mixed liquor recycle ratio and dissolved oxygen on performance of pre-denitrification submerged membrane bioreactors, Water Res., 42 (2008) 1122–1132.
[11] C. Wisniewski, A. Grasmick, Floc size distribution in a membrane bioreactor and consequences for membrane fouling, Colloids Surfaces A: Physicochem. Eng. Asp., 138 (1998) 403–411.
[12] APHA, Standard Methods for Water and Wastewater Examination, American Public Health Association, Washington, DC, 1998.
[13] A. Wachtmeister, T. Kuba, M.C.M. Van Loosdrecht, J.J. Heijnen, A sludge characterization assay for aerobic and denitrifying phosphorus removing sludge, Water Res., 31 (1997) 471–478.
[14] S. Rosenberger, C. Laab, B. Lesjean, R. Gnir, G. Amy, M. Jekel, J.-C. Schrotter, Impact of colloidal and soluble organic material on membrane performance in membrane bioreactors for municipal wastewater treatment, Water Res., 40 (2006) 710–720.
[15] B. Fround, R. Palmgren, K. Keiding, P.H. Nielsen, Extraction of extracellular polymers from activated sludge using a cation exchange resin, Water Res., 30 (1996) 1749–1758.
[16] O.H. Lowery, N.J. Rosebrough, A.L. Farr, R.J. Randall, Protein measurement with the folin phenol reagent, J. Biol. Chem., 193 (1951) 265–275.
[17] G. Belfort, R.H. Davis, A.L. Zydney, The behavior of suspensions and macromolecular solutions in crossflow microfiltration, J. Membr. Sci., 96 (1994) 1–58.
[18] T.H. Bae, T.M. Tak, Interpretation of fouling characteristics of ultrafiltration membranes during the filtration of membrane bioreactor mixed liquor, J. Membr. Sci., 264 (2005) 151–160.
[19] S. Arabi, G. Nakhla, Characterization of foulants in conventional and simultaneous nitrification and denitrification membrane bioreactors, Separ. Purif. Technol., 69 (2009) 153–160.
[20] M. Kumar, S.S. Adham, W.R. Pearce, Investigation of seawater reverse osmosis fouling and its relationship to pretreatment type, Environ. Sci. Technol., 40 (2006) 2037–2044.
[21] T. Maruyama, S. Katoh, M. Nakajima, H. Nabetani, T.P. Abbott, A. Shono, K. Satoh, FT-IR analysis of BSA fouled on ultrafiltration and microfiltration membranes, J. Membr. Sci., 192 (2001) 201–207.
[22] J.P. Croué, M.F. Benedetti, D. Violleau, J.A. Leenheer, Characterization and copper binding of humic and nonhumic organic matter isolated from South Platte River: evidence for the presence of nitrogenous binding site, Environ. Sci. Technol., 37 (2003) 328–336.
[23] A. Ramesh, D.J. Lee, J.Y. Lai, Membrane biofouling by extracellular polymeric substances or soluble microbial products from membrane bioreactor sludge, Appl. Microbiol. Biotechnol., 74 (2007) 699–707.